Engineering and Technology Journal
Journal homepage: https://etj.uotechnology.edu.iq

Comparative Study of Three SAW Configurations for Temperature Sensing

Serhane R., Belkhelfa N.*

Microelectronics and Nanotechnology Division, Center for Development of Advanced Technologies, Cité du 20 Aout 1956, BP 17, Baba Hassen, Algiers, Algeria.
*Corresponding author Email: nbelkhelfa@cdta.dz

HIGHLIGHTS

- Study of three types of Surface Acoustic Wave (SAW) temperature sensors by FEM simulations.
- A theoretical model is developed for temperature change detection when the sensors are subjected to temperature variation.
- The developed model is associated with FEM models used to design a one-port and a two-port SAW resonator added to a delay line sensor.
- A stack of three layers forms the sensors: Si, AlN, and Al.

ARTICLE INFO

Handling editor: Ivan A. Hashim

Keywords:
Coupling factor; Frequency response; Sensors; Surface Acoustic Wave; TCF.

ABSTRACT

This paper demonstrates three SAW configurations' electrical and mechanical behaviors: a one-port resonator, a two-port resonator, and a delay line that works as temperature sensors of around 440 MHz characteristic frequencies. We investigate the sensitivity of the sensors for temperatures up to 200°C. A linear behavior of the frequency shift versus temperature is observed; the resulting sensitivity of the sensors is evaluated at 22.74 ppm/°C for the one-port resonator, 23.17 for the two-port resonator, and 3.83 ns/°C for the delay line structure. The electromechanical coupling coefficient (k^2) is 0.492% for the delay line, 0.489% for the one-port resonator, and 0.55% for the two-port resonator. The quality factor Q_{Factor} calculated from Y_{11} electrical input admittance is 2858 for the one-port resonator, 2977 for the delay line, and 2903 for the two-port resonator. The optimized piezoelectric layer thickness value, for the one port resonator, is h_{AlN}=1.5µm.

1. Introduction

Micro-electro-mechanical system (MEMS) devices have been elaborated and widely used in the last few decades. In research or commercial fields, pressure and temperature sensors are essential areas of MEMS devices. This type of sensor can hardly work in high-temperature situations, like environments where the temperature exceeds 150°C. As a promising solution, the use of acoustic wave technology was adopted. Acoustic wave devices were adopted because of their low cost, small size, low power consumption, and wireless operation principle. Choosing an appropriate design and materials makes these devices sensitive to external conditions, including temperature, pressure, strain, or chemical/biological mass loading [1]. SAW sensors have many features that make them a favorable solution in various sensing applications [2], especially for environmental parameter measurement. Three configurations are mainly used as sensors: the one-port resonator, the two-port resonator [3,4], and the delay line [5, 6]. A stack of semiconductor/piezoelectric/metal layers forms those devices where the top metal layer is patterned as IDTs (Inter Digital Transducers) and Bragg reflectors.

The SAW device is susceptible to perturbations of the piezoelectric substrate due to the variation of the ambient environment's physical parameters, like temperature. The ambient temperature variations would result in a change in the resonance frequency of the SAW resonator or the central frequency of the delay line, and based on this change, the extent of temperature variation can be evaluated.

In general, the thermal effects on the SAW resonators' resonance frequency are due to the change in: i) the geometrical parameters of the device due to the thermal extension of materials (like substrate dimensions), and ii) the physical parameters of

http://doi.org/10.30684/etj.2023.137423.1346
Received 20 December; Accepted 31 January; Available online 20 February 2023
2412-0758/University of Technology-Iraq, Baghdad, Iraq

materials, including density and elastic coefficients. All these parameters affect the acoustic wave velocity and are expressed in the SAW device resonance frequency changes [7].

The one-port or two-port SAW resonators consist of one array of inter-digital transducers (IDTs) working as input and output terminals associated with two grating reflectors placed on both sides of the IDTs and acting as Bragg mirrors. Consequently, an acoustic cavity is created between the reflectors. The transducers (IDTs), when receiving an electrical interrogative signal launch an elastic wave in the cavity. A standing wave is formed because of the interference between the incident and the reflected SAW waves at the resonance frequency [8]. The piezoelectric material converts the elastic wave back to an electrical signal.

The operation principle of a two-port SAW delay line is similar to the SAW resonator. The cavity system in delay line devices works based on the traveling time of the acoustic wave from the transmitter IDTs to the receiver ones. An external perturbation, like pressure or temperature change, leads to a change in the acoustic path and the propagation velocity of the SAW wave; which causes a shift in the phase and consequently a shift in the central frequency of the device. SAW delay line configuration is very important because it is the most obvious application of SAW devices; it has been used to design sensors, filters, and correlators [8].

Many defies must be overcome when elaborating wireless temperature sensors, the main challenges are the legal regulations for industrial, scientific, and medical frequency bands (ISM-bands) [9]; as well as the stability of the sensor. Those challenges impose several restrictions on any system design. The main requirements for SAW sensors are frequency stability and a high-quality factor (Q_{Factor}) [10,11]. The frequency stability can be measured by the temperature coefficient of frequency (*TCF* constant) which describes the change of the resonance frequency in the case of resonators and the change of the central frequency in the case of delay lines when the temperature changes.

The piezoelectric substrate is the key to any sensor design; many parameters define the exploitability of piezoelectric substrates for temperature SAW sensors. Those parameters are the electromechanical coupling coefficient (k^2); the SAW propagation velocity; the mechanical quality factor (Q_{Factor}) and the *TCF* value (it should be large to obtain a maximum sensing effect and hence a high-frequency resolution) [12]. For temperature sensors, of course, the stability of the material itself against decomposition and against loss of the piezoelectric effect when temperature increases is an additional requirement. Many piezoelectric materials have been used in SAW devices, among them Aluminum Nitride (AlN) which was widely used. This piezoelectric material brings many qualities that make it a material of great interest for electronic applications. It has an acoustic phase velocity close to 5700 m.s-1, allowing high-frequency device fabrication (up to 10 GHz). Aluminum Nitride can be used in high-temperature conditions, it melts at 3214°C but decomposes chemically in a vacuum at 1040°C, which induces good chemical and thermal stability. Additionally, it has a good electromechanical coupling coefficient (0.32%) [13,14]. These properties make it perfect for high-frequency SAW applications at high temperatures. Moreover, the fabrication of AlN SAW devices is compatible with the conventional CMOS (Complementary Metal Oxide Semiconductor) technology on silicon.

Actually, and as mentioned above, two basic structures of SAW temperature sensors have been reported in the literature: delay lines and resonators (Figure 1). In the work of Xuesong Ye et al. [15], SAW temperature sensors based on delay line configuration had a phase shift (sensitivity) of 10º/K. However, these SAW sensors had a lower Q_{Factor} than SAW resonator sensors using the same piezoelectric material. Additionally, SAW resonators have the characteristics to impose fewer demands on the substrate's coupling coefficient and allow the fabrication of small sensors [11].

In this work, we study three SAW structure configurations (a one-port resonator, a two-port resonator, and a delay line) that are intended to work as temperature sensors at around 440 MHz central frequencies. This low operation frequency in addition to being inside the ISM bands, allows using any standard material as a piezoelectric substrate; like AlN chosen in our study. Furthermore, the low-frequency choice leads to less loss either in the free field of propagation or on the substrate, which results in relatively wide electrode structures. The increased width of the sensor electrodes enhances their temperature stability [11]. Moreover, the low frequency has a direct effect on the readout circuitry. Low frequency allows the interrogation of the sensors with a read-out positioned at several meters (5-10 meters according to the antenna size). At this frequency, the SAW wavelength is about 10.8 µm thus permitting the usage of simple and small antennas [16].

The theoretical temperature model elaborated to study the temperature effect on the (S_{11} and S_{21}) parameters is described and the equations constituting the model are detailed. Those equations express the influence of the temperature on the materials' physical and geometrical parameters.

The performances of the designed Al/AlN/Si temperature sensors at different temperatures are investigated. The (S) scattering parameters (S_{11} reflection coefficient and S_{21} transmission coefficient) of the sensors are calculated. Those parameters are characterized by a shift in the central frequency (delay line configuration case) and the resonance frequency (resonator configuration case) toward law values when temperature changes; the sensitivity of the sensors is evaluated using these shifts.

The electromechanical coupling coefficient (k^2) and the quality factor (Q_{Factor}), for the three configurations, are evaluated. An IFFT (inverse fast Fourier transform) is performed on S_{11} and S_{21} signals of the delay line structure, and the effect of temperature variation on the delay time (τ) is studied. After that, the effect of the acoustic path (D_{Delay}) on the sensor's sensitivity is investigated. Finally, the influence of the piezoelectric layer thickness (h_{AlN}) on the one-port SAW resonator characteristics is studied; this permits to choose an optimized piezoelectric layer thickness.

2. Studied Structures

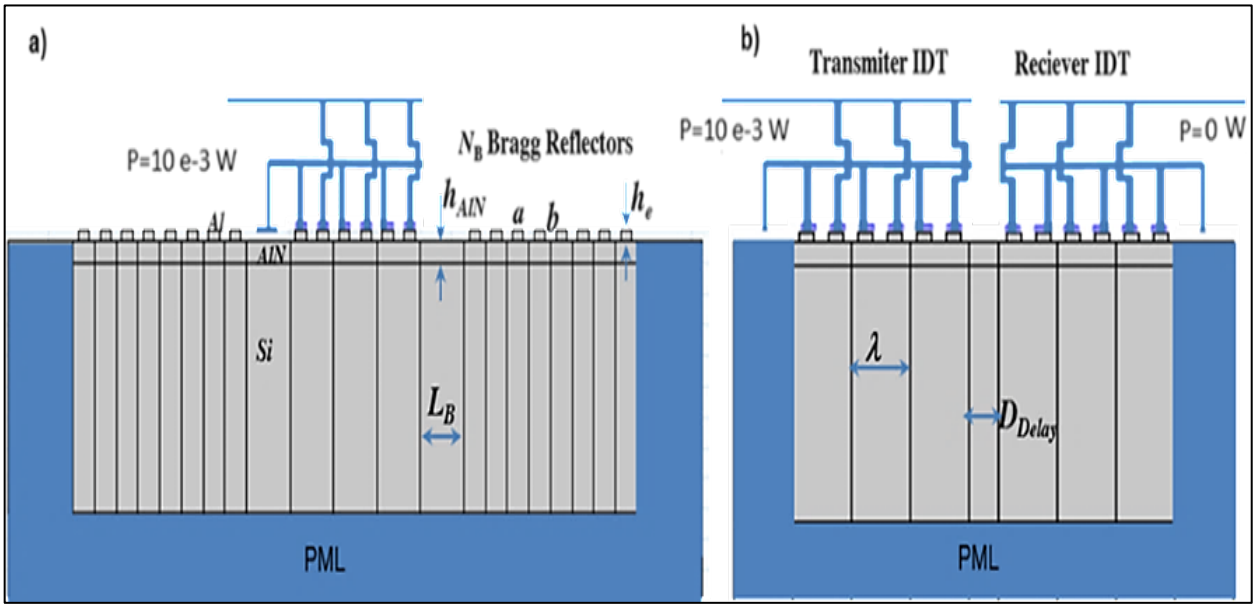

Figure 1: 2D Schematic representation of the studied structures: a) One port SAW resonator and b) SAW Delay line

The geometry of two of the studied SAWs is shown in Figure,1 (namely the one-port resonator and the delay line), they are formed of an AlN piezoelectric layer (which thickness is h_{AlN}=1.5µm), deposited on a (100) silicon substrate. The aluminum inter-digital electrodes (IDTs) have a thickness of 500 nm, the width of the electrodes (a) and the spacing between them (pitch (b)) are 2.7 µm each; the resulting distance between electrodes is then $d=a+b$, and the Rayleigh mode wavelength is $\lambda=2d$=10.8 µm [17]. The number of the transmitter and the receiver electrodes pairs is set to 16 and the distance between the transmitter and receiver ports is $D_{Delay}=\lambda/2$; it represents the free acoustic path causing the SAW wave delay. The number of Bragg reflectors for the SAW resonator is set to 36; they are made of Al. Perfectly matched layers (PML zones) surround the structures to eliminate all unwanted reflections on the lateral or bottom sides.

3. Materials Constituting the Structures

The physical parameters for each material constituting the SAW structures are defined before starting the calculation and for every chosen physic. Among those physical parameters, we can cite: the dielectric permittivity, Young's modulus, volume density, elasticity tensor, piezoelectric tensor,etc. The aluminum forming the IDT electrodes is an isotropic material, its density is 2700 kg/m^3, its Young modulus is 70 GPa and its Poisson's ratio is 0.35. The density of the piezoelectric AlN layer is 3260 kg/m3; the elastic constants : c_{11}, c_{33}, c_{12}, c_{13}, and c_{44} , respectively, equal 410 GPa, 389 GPa, 149 GPa, 99 GPa, and 125 GPa. The piezoelectric constants of AlN are; e_{15}=-0.48 C/m^2, e_{13}=-0.58 C/m^2, and e_{33}=1.55 C/m^2, and its relative dielectric permittivity constants are $\varepsilon_{11}=\varepsilon_{22}$=9 and ε_{33}=11. Silicon constituting the substrate is also considered as an anisotropic material (Mono crystal) with c_{11}=166 GPa, c_{12}=64 GPa and c_{44}=80 GPa, its density is 2330 kg/m^3 [18, 19]. The electrical losses in metallic regions (originating from the Joule effect) are neglected. Still, the mechanical and dielectric losses are considered in the model using complex values of the elasticity matrix (c_E) and complex values for the dielectric permittivity tensor (ε_S), according to (1) and (2) respectively [20]:

$$c_E^{(i,j)} = (1 + j\eta_{cE}^{(i,j)})c_E^{(i,j)} \quad (1)$$

$$\varepsilon_S^{(i,j)} = \left(1 - j\eta_{\varepsilon S}^{(i,j)}\right)\varepsilon_S^{(i,j)} \quad (2)$$

η_{cE}=0.5 10^{-3} in AlN, 0.2 10^{-3} in Al and 0.166 10^{-3} in Si, and the dielectric losses in AlN are $\eta_{\varepsilon S}$=0.02.

4. Boundary Conditions

4.1 Electrical Boundary Conditions (Grounds, Terminals)

For S-parameters determination, we consider the entire SAW structures in Figure 1a and Figure 1b, where electrical power is applied to the devices. In the case of a one-port SAW resonator, an electrical power of 10 mW is applied to the IDTs, and only the S_{11} reflection parameter is calculated which represents the return losses. In the case of a delay line configuration, the input IDTs (transmitter) is set to a power of 10 mW (they form terminal 1) and the output IDTs (receiver) are set to a power of P=0 W (Terminal 2), both S_{11} (reflection) and S_{21} (transmission) parameters are calculated representing respectively the return losses and the insertion losses.

4.2 Mechanical Boundary Conditions

The numerical simulation of wave propagation problems in an infinite media, using the finite element method FEM, requires the reduction of the medium of study into a truncated domain (or reduced zone). For a complete SAW structure of finite dimensions, and in order to avoid edge effects at the free ends of the field of study, we consider the absorbent layer method, which is one of the most widely used techniques. It consists of finite thickness layers called PML (Perfectly Matched Layers), which surround the boundaries of the field of study (lateral and bottom sides) in order to force the waves to dampen by traveling a given distance in the absorbent domain. Figure 1. a.b shows the absorbing PML regions in the case of one-port resonator and delay line SAW structures. The lateral and bottom extremities of both structures are set to a fixed constraint (i.e. zeros mechanical displacement amplitude).

5. Description of the Temperature Sensing Model

A theoretical temperature model is implemented in Comsol, this model uses equations describing the variations of the sensor's physical and geometrical parameters with temperature.

The influence of the temperature on the resonance frequencies of the SAW devices is given by the *TCF* constant, which is the temperature coefficient for frequency; it permits the evaluation of the SAW's resonance frequency normalized shift (in ppm, part per million) for a 1°C variation in temperature *T* [21].

$$TCF = \frac{1}{f_0}\frac{\partial f_0}{\partial T} \tag{3}$$

In the case of SAW-based temperature sensors, a large value of the *TCF* constant is very beneficial because this *TCF* is also the sensitivity *S* [ppm/°C] of the sensor (*S*=*TCF*).

This sensitivity can also be expressed without normalization by *s*[Hz/°C], according to (4):

$$s = \frac{\partial f_0}{\partial T} \tag{4}$$

5.1 Parameters Influencing the TCF Constant

As described before, for an elementary temperature variation, the *TCF* constant links directly to the relative change in the resonance frequency (3). However, the resonance frequency f_0 relates to the surface wave velocity (V_{SAW}) and the pitch (d) of the inter-digital transducers as follows:

$$f_0 = V_{SAW}/2d \tag{5}$$

The relative change in the resonance frequency due to temperature change can be expressed as a function of the two relative changes in acoustic velocity and the distance *d*, as expressed in (6) [19]:

$$TCF = \frac{1}{v_{SAW}}\frac{\partial v_{SAW}}{\partial T} - \frac{1}{d}\frac{\partial d}{\partial T} = TCV - \alpha \tag{6}$$

With

$$TCV = \frac{1}{v_{SAW}}\frac{\partial v_{SAW}}{\partial T} \tag{7}$$

$$\alpha = \frac{1}{d}\frac{\partial d}{\partial T} \tag{8}$$

TCV is the temperature coefficient for the velocity, α is the thermal expansion constant of the substrate.

In this conventional approach, we consider that the (thicker) substrate can force the elongation of the above (thinner) AlN and Al layers; this means that the thermal coefficient (equation 8) is that of the substrate (Si).

Similarly, the wave velocity is a function of the elastic constants c_{ij}^{D} and the denity ρ of the propagation medium ($v_{SAW}=\sqrt{c_{ij}^{D}/\rho}$), so its relative variation can be expressed as follows:

$$TCV = \frac{1}{2}\left(\frac{1}{c_{ij}^{D}}\frac{\partial c_{ij}^{D}}{\partial T} - \frac{1}{\rho}\frac{\partial \rho}{\partial T}\right) = \frac{1}{2}\left(TCE - \frac{1}{\rho}\frac{\partial \rho}{\partial T}\right) \tag{9}$$

With,

$$TCE = \frac{1}{c_{ij}^{D}} \frac{\partial c_{ij}^{D}}{\partial T} \tag{10}$$

This represents the temperature dependence of the elastic constants. The calculation of density relative change in (9) is only a matter of material dilatation in all directions:

$$\frac{1}{\rho} \frac{\partial \rho}{\partial T} = -(\alpha_{11} + \alpha_{22} + \alpha_{33}) \tag{11}$$

Where α_{11}, α_{22}, and α_{33} represent the effective thermal expansion coefficients of the piezoelectric layer in the *x*, *y,* and *z* directions, respectively. By replacing (11) in (9) and then in (6), the constant *TCF* becomes:

$$TCF = \frac{1}{2}\left[TCE - (\alpha_{11} + \alpha_{22} + \alpha_{33})\right] - \alpha \tag{12}$$

Thus, the change in the temperature of the surrounding environment can cause four distinct effects:
i) A change in the length of the propagation path (case of the delay line),
ii) a change in the SAW wavelength caused by the inter-digital distance *d* modification,
iii) a change in the density when the material is elongated or dilated,
iv) a change in the elastic constants under thermal stress.

5.2 Parameters to be Considered in FEM Simulation of a SAW Temperature Sensor

When constructing a model for SAW temperature sensors by the Finite Element Method (FEM), one must consider the variations of the physical and geometrical parameters due to the change in temperature *T* as follows (they are developed in the first order) [22, 23]:

$$d = d(T_0)(1 + \alpha.\Delta T) \tag{13}$$

$$h_{AlN} = h_{AlN}(T_0)(1 + \alpha_{33}\Delta T) \tag{14}$$

$$\rho(T) = \rho(T_0)\left[1 - (\alpha_{11} + \alpha_{22} + \alpha_{33})\Delta T\right] \tag{15}$$

The elastic constants developed in the second order are:

$$c_{ij}(T) = c_{ij}(T_0)\left[1 + TCE_{ij}\Delta T + TCE2_{ij}\Delta T^2)\right] \tag{16}$$

$$D_{\text{Delay}}(T) = D_{\text{Delay}}(T_0).\ (1 + \alpha.\Delta T) \tag{17}$$

For AlN, Si, and Al, constants α_{11}, α_{22}, α_{33}, TCE_{ij}, and $TCE2_{ij}$ are summarized in Table 1.

6. Results and Discussion

6.1 Two Ports Delay Line Configuration

To predict the behavior of the studied delay line structure with temperature variation, the SAW device *S* parameters (S_{11} return losses and S_{21} insertion losses) are evaluated in the frequency domain, for temperatures varying from -25°C to 200°C and by using the elaborated theoretical model. After that, we performed an inverse fast Fourier transform (IFFT algorithm) on the set of S_{11} and S_{21} data to obtain the time-domain representation.

In Figure 2, the total mechanical displacement field of the delay line at the central frequency (f_0=444.8 MHz) is represented. One can notice that at this frequency, the maximum energy is confined at the top surface of the structure, which means that the Rayleigh mode is generated at this frequency. At this frequency as well, the S_{11} parameter Figure 3a exhibits a minimal value (-0.02 dB), and the S_{21} parameter is at its maximal value Figure 3c.

The reflection coefficient variation curves $S_{11}(f)$ for temperatures T ranging from -25°C to 175°C with a step of 50°C are shown in Figure 3a. The reflection parameter S_{11} shifts toward low frequencies and its magnitude decrease very slightly with temperature. The temperature behavior of S_{11} is attributed to the thermal expansion, which would enlarge finger size (*a*) and spacing (*b*), and consequently causes the increase of the wavelength (since λ=2(*a*+*b*)). The increase of the wavelength would decrease the frequency according to (5). The transmission coefficient $S_{21}(f)$ is also represented in Figure 3c, for temperatures *T* ranging from -25°C to 175°C with a step of 50°C. (S_{21}) magnitude does not change with temperature, but it also shifts slightly toward low frequencies when the temperature increases.

Table 1: Physical parameters of AlN, si, and Al used in the FEM model [24, 25]

		AlN	Si	Al
Elastic constants, c_{ij} [GPa]	c_{11}	410.06	170	70
	c_{12}	100.69		
	c_{13}	83.82		
	c_{33}	386.24		
	c_{44}	100.58		
	c_{66}	154.70		
1st order TCE TCE_{ij} [10^{-6}/K]	Tc_{11}	-10.65	-63	-
	Tc_{12}	-11.67		
	Tc_{13}	-11.22		
	Tc_{33}	-11.13		
	Tc_{44}	-10.82		
	Tc_{66}	-10.80		
2nd order TCE $TCE2_{ij}$ [10^{-9}/K^2]	$T2c_{11}$	-20.61	-52	-
	$T2c_{12}$	-19.51		
	$T2c_{13}$	-19.88		
	$T2c_{33}$	-20.03		
	$T2c_{44}$	-20.36		
	$T2c_{66}$	-20.39		
Piezoelectric stress coef., e_{ij} [C/m^2]	e_{15}	-0.48	-	-
	e_{31}	-0.58		
	e_{33}	1.55		
Relative permittivity, ε_{ij}	ε_{11}	9	11.7	-
	ε_{33}	11	11.7	
CTE, α_{ij} [10^{-6}/K]	α_{11}	5.27	2.6	18
	α_{33}	4.15	2.6	18
Density, ρ [kg/m^3]		3260	2329	2700

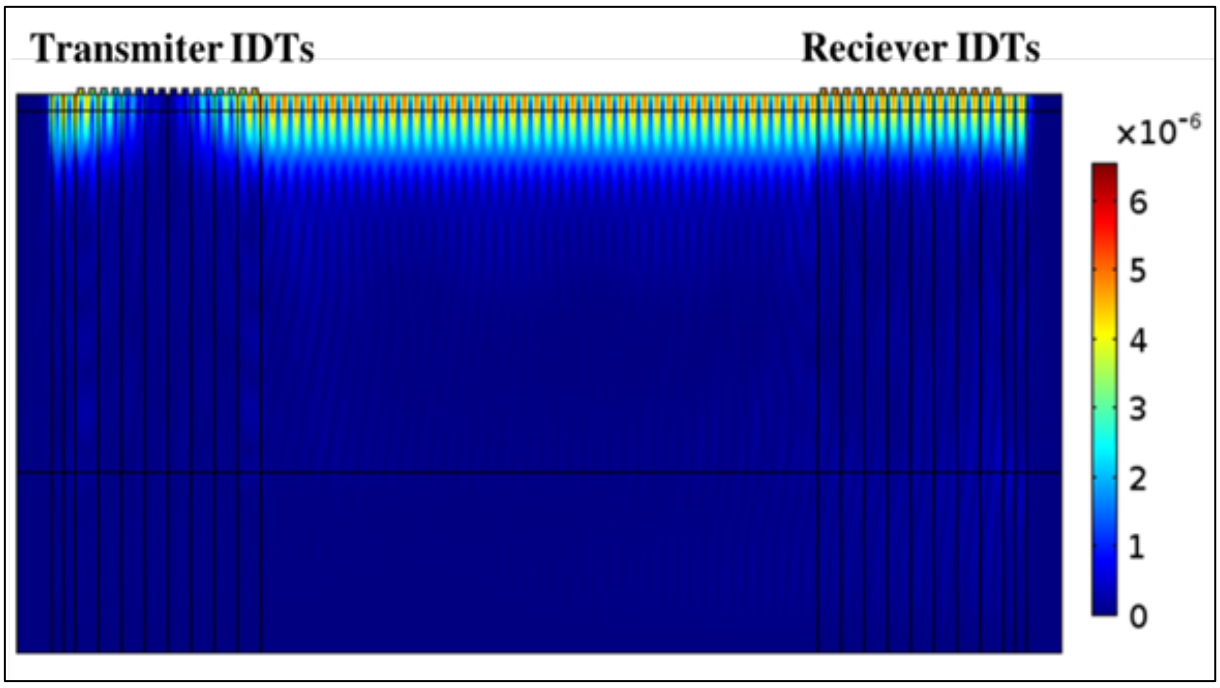

Figure 2: Total mechanical displacement field of the delay line at the central frequency f0= 444.8 MHz

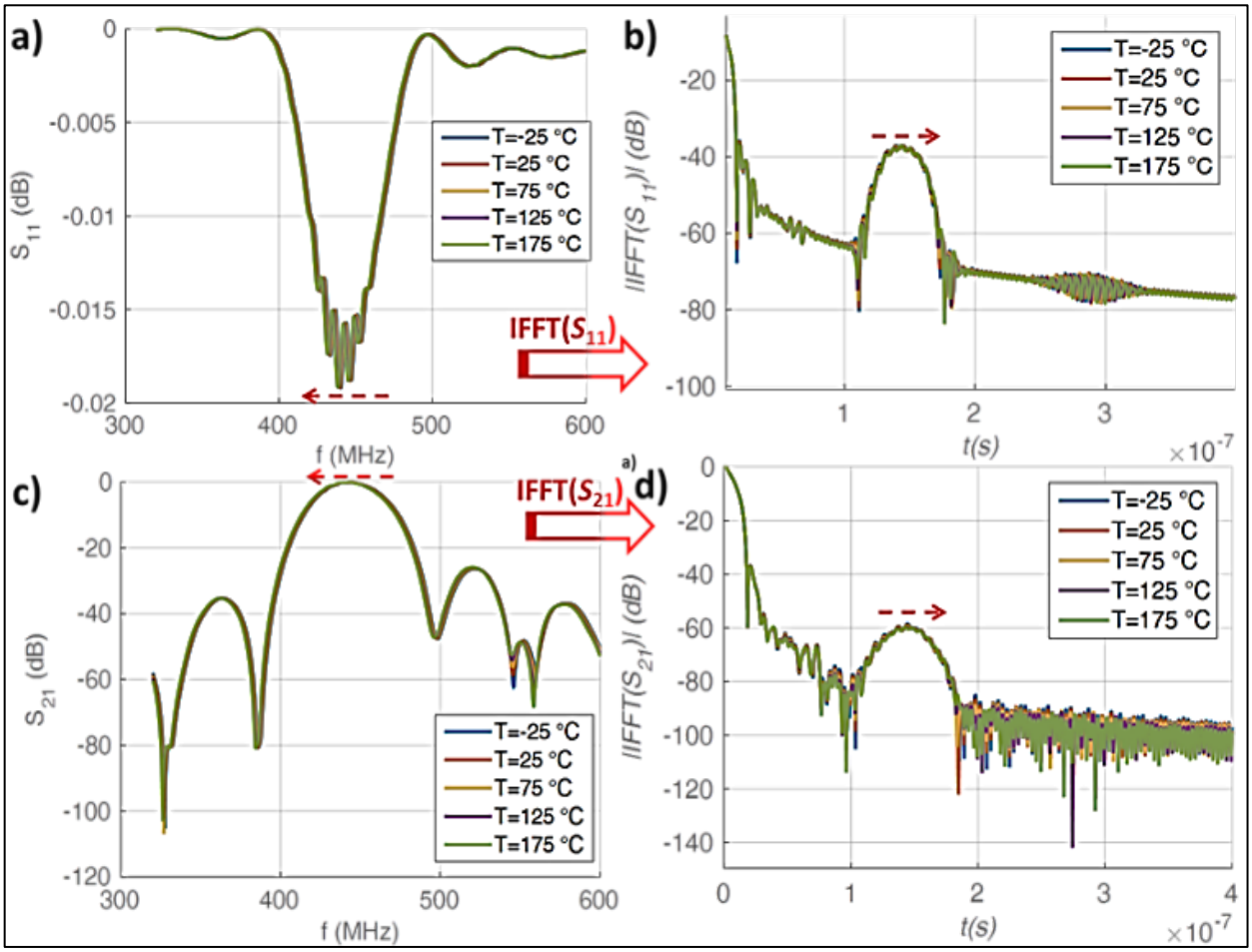

Figure 3: Delay line SAW temperature sensor electrical response (operating frequency 444.8 MHz), a)-Reflection parameter S11(f) and b)-IFFT(S11(f)), c)-Transmission parameter S21(f), and d)- IFFT(S21 (f))

An IFFT is performed on $S_{11}(f)$ and $S_{21}(f)$ signals to represent them in the time domain, the corresponding $S_{11}(t)$ and $S_{21}(t)$ are represented in Figure 3b and Figure 3d respectively.

For the determination of the delay (τ) values, the zero-padding algorithm is used. In fact, the achievable precision of the applied IFFT was not adequate for delay time measurement, and this resolution was enhanced by increasing the sampling frequency (f_s) by adding zeros to the calculated data (zero padding). Since the resolution of the time axis, Δt is inversely proportional to the sampling frequency (f_s) of the RF measurement $(\Delta t=1/f_s)$, increasing f_s would increase the precision.

The maximum of the first reflected pulse Figure 3b and the first transmitted pulse Figure 3d is obtained at $t=0.145\mu$s. It represents the delay time (τ) defined as the time taken by the wave to travel the acoustic path (24λ in this case) with a velocity V_{SAW}. This delay time increases when the length of the acoustic path increases as demonstrated in Figure 4a. It is notable that D_{Delay}=60λ gives higher delay time than D_{Delay}=48λ or D_{Delay}=24λ.

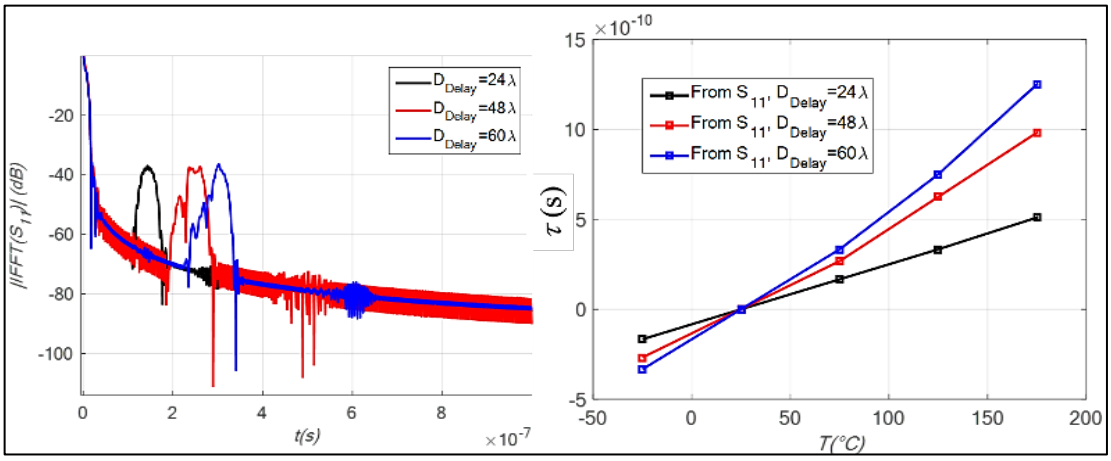

Figure 4: a)-S11(t) for different lengths of the SAW path (DDelay),b)- Delay time shift versus temperature (sensitivity of the delay line)

The effect of the temperature's increase on the acoustic path or the delay time is investigated in Figure 3b and Figure 3d. It appears that S_{11} and S_{21} delays (τ) are increasing with temperature. This can be explained by the fact that when temperature increases, the acoustic path undergoes a dilatation that induces an increase in the delay. This (τ) variation with temperature was evaluated and it is shown in Figure 4b (the black line); it exhibited a linear increase while temperature grew up to 175°C.

The slope of τ variation versus temperature ($\tau(T)$) line, gives the sensitivity of the delay line, and by using the formula

$$S_{Delay}=2\pi f_0 \tau \tag{18}$$

A slope of 3.83 ns/°C is obtained from the black line ($D_{Delay}=24\lambda$) of Figure 4b. In order to check the effect of the acoustic path on the sensitivity of the sensors, the same study is performed on structures with $D_{Delay}=48\lambda$ (red line) and $D_{Delay}=60\lambda$ (blue line). Sensitivities of 6.25 ns/°C and 7.92 ns/°C were obtained for each structure respectively.

6.1.1 Electromechanical coupling coefficient

The electromechanical coupling coefficient ($Keff^2$) is an inherent characteristic of the SAW device; it measures the electrical energy conversion ratio into a mechanical one by piezoelectric transduction effect. This factor is determined from the electrical input admittance curve $Y_{11}(f)$ of the sensor (at ambient temperature) using the Equation:

$$k_{eff}^2 = \frac{\pi}{4N_p}\frac{Real(Y_{11})}{Imag(Y_{11})}\Big|_{f=f_0} \tag{19}$$

The calculated k^2 for the delay line configuration is 0.492% at the center frequency f_0=444.8 MHz.

6.1.2 Quality factor of the device

The quality factor Q_{Factor} of the sensor can be deduced in COMSOL, at all frequencies, by using the following equation [20]:

$$Q_{Factor} = 2\pi\frac{W_h}{Q_h}\Big|_{f=f_0} \tag{20}$$

Where Q_h is the energy lost in one cycle, and W_h is the maximum of the potential energy stored in the cycle. At the central frequency of the delay line f_0=444.8 MHz and at ambient temperature, the quality factor value for the studied structure is evaluated at Q_{Factor}=2977.

6.2 One Port Resonator Configuration

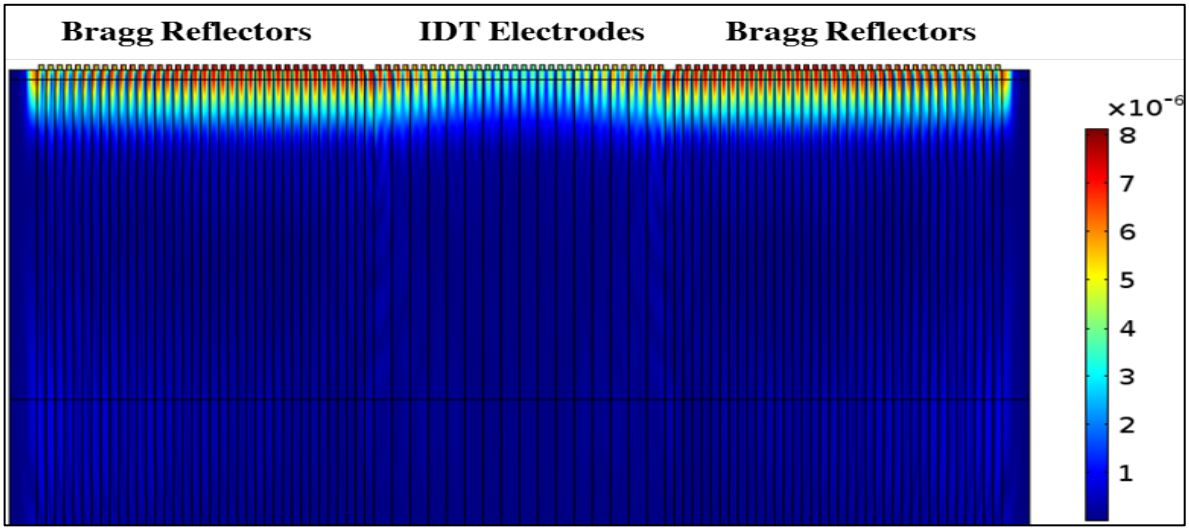

Figure 5: Mechanical displacement field at the resonance frequency of the single-port SAW temperature sensor operating at a frequency of f0= 440 MHz

At T=25°C, the SAW resonator exhibits a resonance frequency at f_0=440 MHz. The quality factor at this frequency is Q_{Factor}=2858, and the electromechanical coupling coefficient is K_{eff}^2=0.489%.

The mechanical displacement field of the studied structure at the resonance frequency is represented in Figure 5. One can notice that: *i*) most of the sensor energy is confined in the top surface of the structure (in a depth less than 1.5λ) which is a SAW Rayleigh mode characteristic, and *ii*) the Bragg system constitutes an acoustic resonant cavity where the acoustic energy is confined laterally between the two mirror reflectors systems.

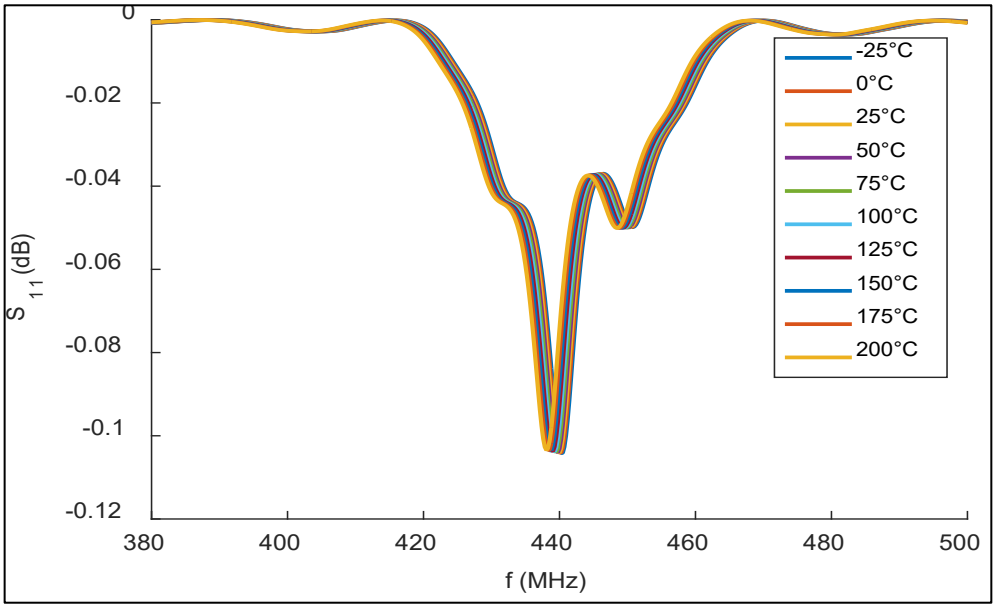

Figure 6: Single port SAW temperature sensor electrical response, at 440 MHz

In Figure 6, $S_{11}(f)$ is represented. The resonance frequency shifts toward low frequencies when temperature increases and the S_{11} parameter magnitude decreases a bit. The shift of the resonance frequency (f_0) as a function of temperature is represented in Figure 7; the sensor sensitivity is calculated from the slope of the linear fit performed on the represented data. The sensitivity is estimated at s=-10 kHz/°C, it corresponds to S=22.74 ppm/°C.

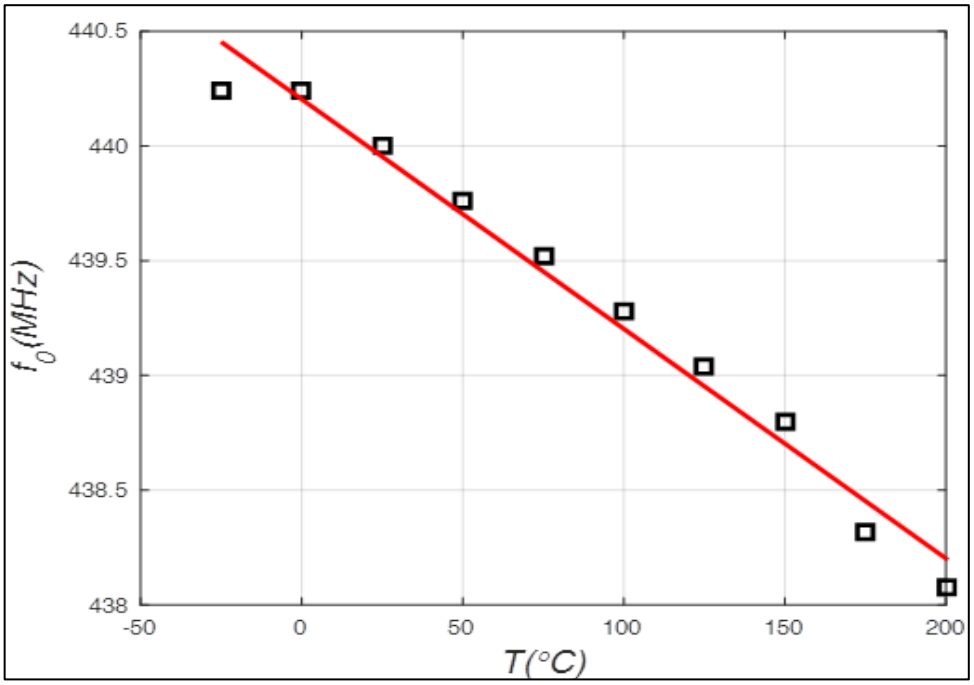

Figure 7: Resonance frequency variation versus temperature of the one port SAW sensor

6.3 Two Ports Resonator Configuration

At T=25°C, the SAW two ports resonator exhibits a resonance frequency at f0=441 MHz. The quality factor at this frequency is QFactor=2903, and the electromechanical coupling coefficient is keff 2=0.55%.

The mechanical displacement field of the studied two ports resonator at the resonance frequency (f0=441 MHz) is represented in Figure 8. Most of the sensor energy is confined in the top surface of the structure; it is mainly confined laterally between the two ports of the Bragg reflectors.

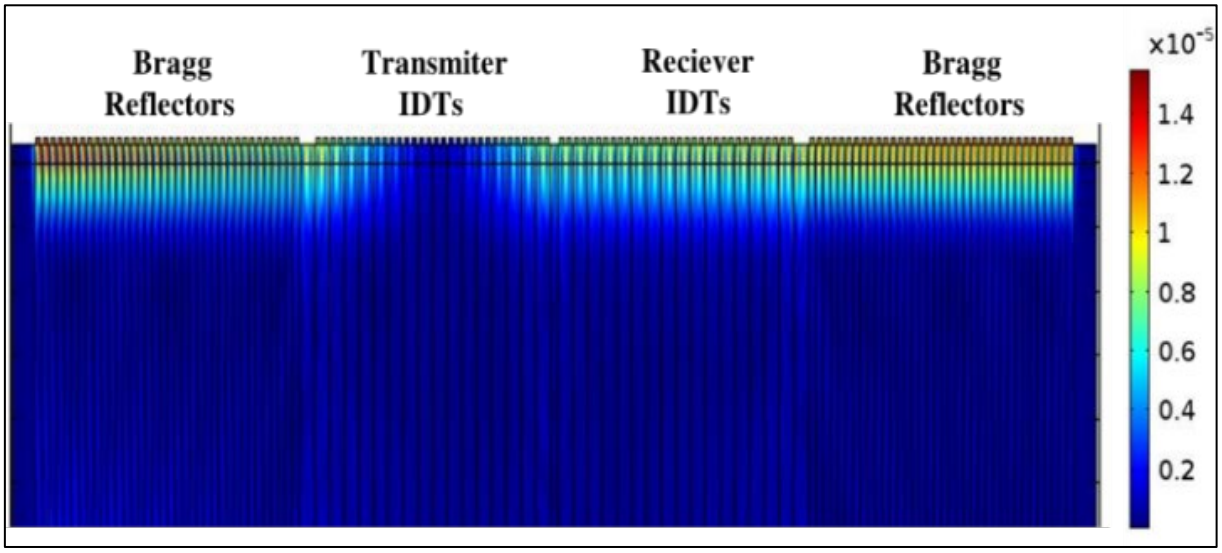

Figure 8: Mechanical displacement field at the resonance frequency of the two-port resonator SAW temperature sensor operating at a frequency f0 = 441 MHz

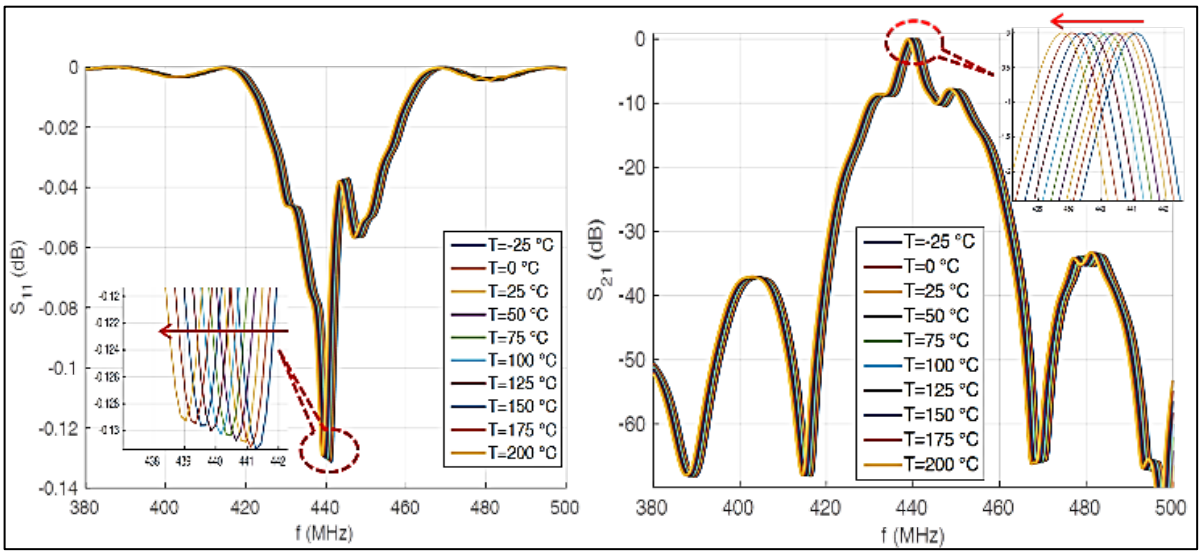

Figure 9: Electrical response of the two ports resonator SAW temperature sensor (operation frequency 441 MHz), a) – S11(f) Reflection coefficient and b)- S21 (f) Transmission coefficient

The reflection coefficient variation curves $S_{11}(f)$ for temperatures T ranging from -25°C to 200°C with a step of 25°C are shown in Figure 9a. In this figure, $S_{11}(f)$ shifts toward low frequencies and its magnitude decrease slightly with temperature. The transmission coefficient $S_{21}(f)$ is also represented in Figure 9b, for temperatures T ranging from -25°C to 200°C with a step of 25°C. S_{21} magnitude does not change with temperature, but it also shifts toward low frequencies when temperature increases.

The shift of the resonance frequency (f0) as a function of temperature is shown in Figure 10. The sensor sensitivity is calculated from the slope of the linear fit performed on the data obtained from the S11 and S21 parameters. The sensitivity, calculated from the slope of the resonance frequency variation with temperature obtained from the S11 curve, was estimated at s=-10.22 kHz/°C (it corresponds to S=23.17 ppm/°C). This sensitivity was evaluated at s=-10.66 kHz/°C (S=24.17 ppm/°C) from the slope of S21 resonance frequency variation with temperature. This means that the use of either S11 or S21 parameters for sensitivity evaluation is possible.

The obtained values of sensitivities for the delay line, the one-port resonator, and the two-port resonator sensors are summarized in Table 2.

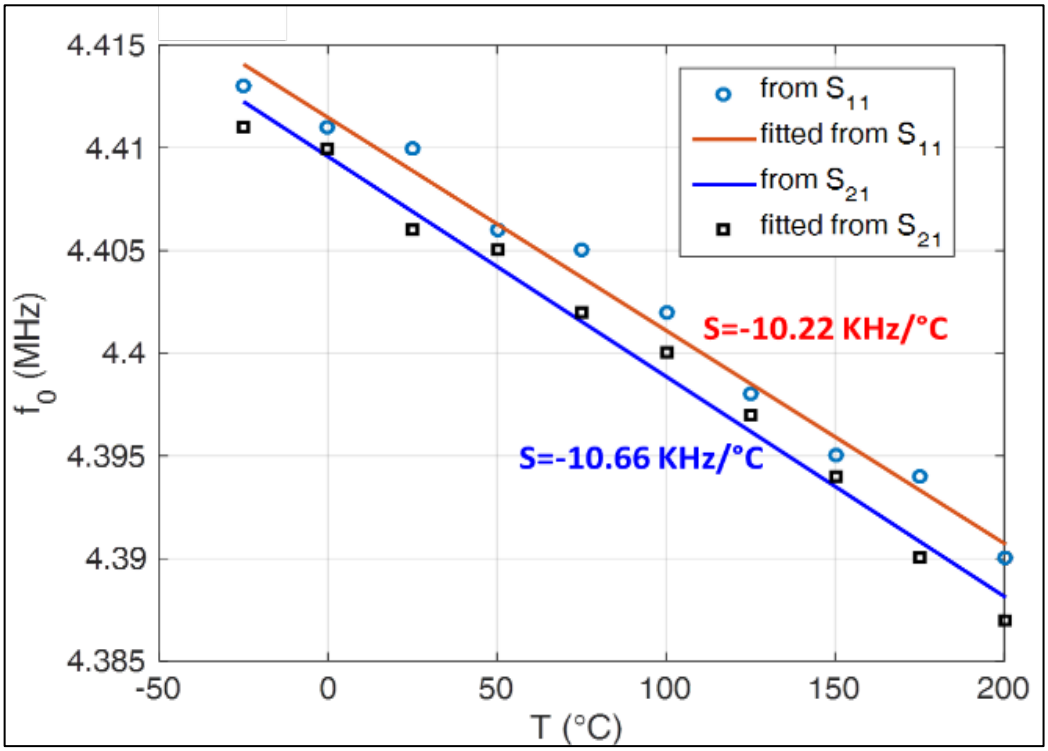

Figure 10: Resonance frequency variation versus temperature of two ports resonator SAW temperature sensor (working frequency 441 MHz)

Table 2: Results obtained with the three saw sensors configurations

Delay line (444.8 MHz) SAW Temperature sensor Al/AlN/Si (vs D_{Delay})		**One port resonator (440 MHz) SAW Temperature sensor Al/AlN/Si**		**Two ports resonator (441 MHz) SAW Temperature sensor Al/AlN/Si**	
D_{Delay}	***s (10^{-9}s/°C)***	***s (kHz/°C)***	***S (ppm/°C)***	***s (kHz/°C)***	***S (ppm/°C)***
24λ	3.83				
48λ	6.25	-10	22.74	10.22 from S_{11} 10.66 from S_{21}	23.17 24.17
60λ	7.72				
k^2	***Q***	***k^2***	***Q***	***k^2***	***Q***
0.492%	2977	0.489%	2858	0.55%	2903

7. Effect of Piezoelectric Layer Thickness (hAlN) on SAW Resonator Characteristics

The piezoelectric layer thickness is an important parameter to consider when designing a SAW sensor. The thickness of 1.5µm adopted in the ongoing study was deduced from a previous one, in which the objective was the SAW sensor geometrical parameters optimization [26]. In order to further the investigations, we study in the following the effect of AlN thickness (h_{AlN}) on the sensitivity of the one-port SAW resonator sensor. The aim is to choose the (h_{AlN}) that gives a good sensitivity added to an acceptable piezoelectric effect. To perform this study, three temperature values are investigated 0°C, 100°C, and 200°C. The thickness of the AlN layer was varied from 0.5 µm to 3 µm with a step of 0.5 µm for each value of the studied temperature. Figure 11 represents the variation of the S_{11} reflection parameter when varying AlN thickness; each AlN thickness is represented for three values of the temperature. According to Figure 11, the S_{11} reflection coefficient magnitude increases when AlN layer thickness rises (the smallest curves are obtained with h_{AlN} = 0.5 µm and the biggest ones are obtained with h_{AlN}=3 µm) ; this would induce an improvement in both the electromechanical coupling coefficient and the quality factor.

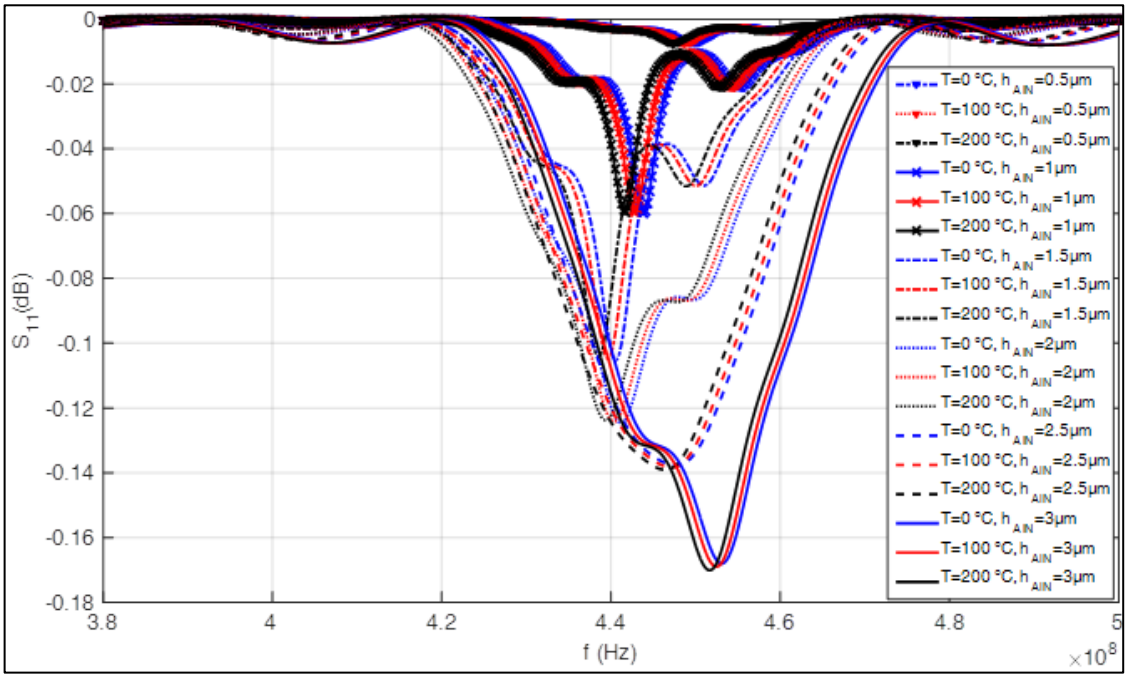

Figure 11: Effect of AlN layer thickness (hAlN) on SAW resonator S11 characteristics for three values of temperature

Variation of the SAW temperature sensor sensitivity with h_{AlN} is shown in Figure 12; this sensitivity decreases when h_{AlN} rises. h_{AlN}=1 µm and 0.5 µm give a better sensitivity compared to h_{AlN}=1.5 µm ("Figure12"), but regarding S_{11} intensity Figure 11, the S_{11} magnitude obtained with h_{AlN}=1.5 µm is higher than that obtained with h_{AlN}=1 µm and 0.5µm. Among the most critical requirements while designing a SAW sensor is to have at the same time reasonable sensitivity and piezoelectric response. In order to satisfy this requirement, h_{AlN}=1.5 µm is chosen as the best compromise to obtain relatively a rational sensitivity (10 kHz/°C) and an acceptable piezoelectric effect (S_{11} magnitude around -0.11 dB).

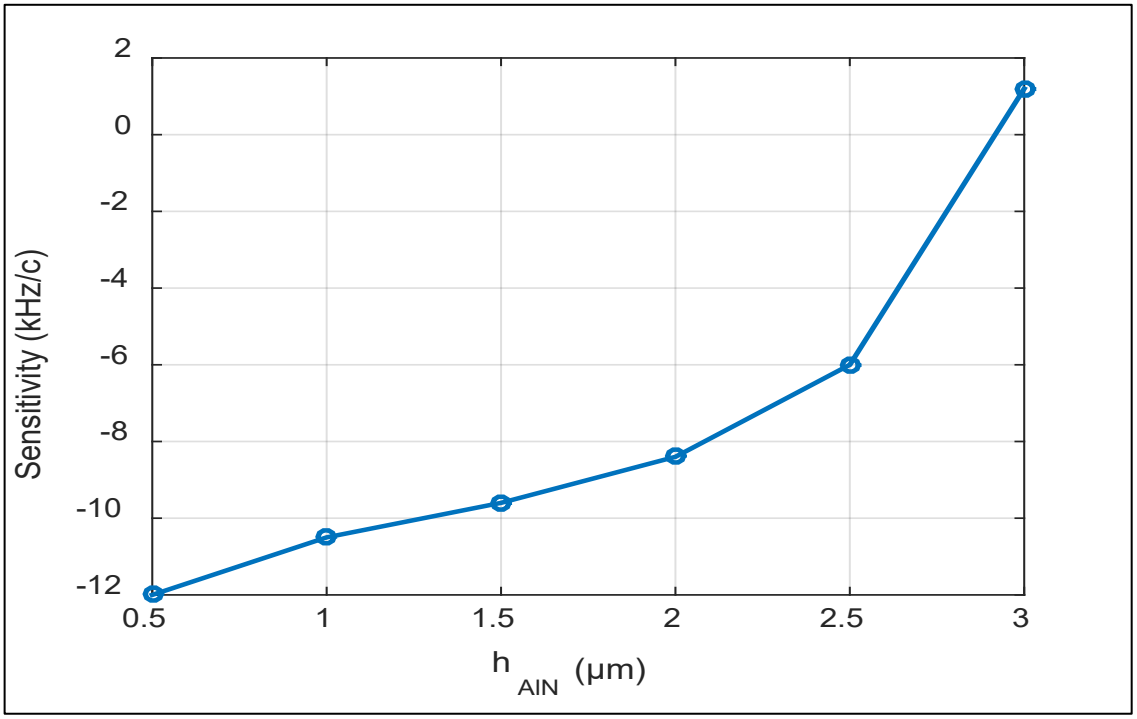

Figure 12: Sensitivity of one port SAW temperature sensor versus h_{AlN} thickness

8. Conclusion

In this work, we have described the theoretical model elaborated for the investigation of SAW devices' characteristics modification when they undergo temperature variation. The equations constituting the model were detailed; those equations express the influence of the temperature on the materials' physical and geometrical parameters.

The model of the SAW structure (FEM model) was coupled with the elaborated temperature model to build a complete digital model of SAW sensors able to predict their behavior when subjected to temperature variation.

Three types of sensor structures were considered, the one-port resonator, the two-port resonator, and the delay line, with a geometry that allows them to be excited at around 440 MHz frequency.

To evaluate the frequency versus temperature behavior of the studied structures, the reflection (S_{11}) and transmission (S_{21}) characteristics of the delay line and two-port resonator were calculated. For the one-port resonator, the reflection characteristic (S_{11}) was calculated. The temperature was varied from -25 to 175°C for the delay line study and from -25 to 200°C for the one-port and two-port resonators investigations. The study was performed by using the elaborated theoretical model. The results showed that the variation of frequency with temperature exhibits a correct linear behavior. The sensitivity of the one-port and two-port resonator sensors was calculated at around 23 (ppm/°C). It was around 3.6, 6.2, and 7.7 ns/°C for the delay line sensor, it varied according to the D_{delay} value variation (D_{Delay}=24λ, 48λ, 60λ). The (k^2) coefficient was 0.492%, 0.489%, and 0.55% for the delay line, the one-port resonator, and the two-port resonator structures, respectively. The quality factor was 2977 for the delay line, 2858 for the one-port resonator, and 2903 for the two-port resonator. The effect of AlN thickness on the sensitivity of the one-port resonator was studied, a thickness of h_{AlN}=1.5 µm was adopted by making a compromise between having an acceptable sensitivity added to a satisfactory piezoelectric effect.

Both studied SAW resonator configurations provide adequate, quasi-constant temperature sensitivity, which makes them suitable for temperature sensor applications. The sensitivity obtained with the delay line is smaller, but by considering the quality factor and the electromechanical coupling factor, the three configurations present good values of these latter and the performances of the three studied structures seem satisfactory for being used as temperature sensors.

Author Contributions

All authors contributed equally to this work.

Funding

This research was supported by Ministère de l'enseignement supèrieur et de la recherche scientifque and funded by Direction Générale de la Recherche Scientifique et du Développement Technologique (DGRSDT), Algeria, grant number: 05/CDTA/DGRSDT/2017, CT-SAW/CMOS 1 µm project. The funders had no role in the design of the study; in the collection, analyses, or interpretation of data; in the writing of the manuscript, or in the decision to publish the results.

Data Availability Statement

The data that support the findings of this study are available on request from the corresponding author.

Conflicts of Interest

The author declares that there're no conflicts of interest for declaration.

References

[1] R. Serhane, F. Hadj Larbi, A. Smatti, FEM Modeling of Sensitive Layer Swelling Effect on Microbalance Gas Sensor Based on TFBAR Resonator, J. Mater. Sci. Appl., 1 (2015) 161–167.

[2] E. Blampain, O. Elmazria, T. Aubert, B. Assouar, O. Legrani, Surface Acoustic Wave sensor based on AlN/Sapphire structure for high temperature and high frequency applications, SENSORS, 2011 IEEE, Limerick, Ireland, 2011, 610-613. https://doi.org/10.1109/ICSENS.2011.6126984

[3] A. S. Shvetsov, S A. Sakharov, O. Elmazria, High Temperature SAW Resonator Sensors: Electrode Design Specifics, IEEE Trans. Ultrason. Ferroelectr. Freq. Control. TUFFC, (2017) 08447.

[4] J. Kuhn, F. Möller,SAW resonator temperature sensor, Sens. Actuator A Phys., 30 (1992) 73–75.https://doi.org/10.1016/0924-4247(92)80199-D

[5] N. Ramakrishnana, A. K. Namdeob, H. B. Nemadeb, R. P. Palathinkalb, Simplified Model for FEM Simulation of SAW Delay Line Sensor, Procedia Eng., 41 (2012) 1022–1027. https://doi.org/10.1016/j.proeng.2012.07.278.

[6] M. M. Elsherbini, M. F. Elkordy, A. M. Gomaa, Towards a Simple Model for SAW Delayline Using CAD, American J. Circuits, Syst. Signal Process., 1 (2015) 86–92.

[7] L. Shu, B. Peng, Z. Yang, R.Wang, S. Deng, X. Liu, High-Temperature SAW Wireless Strain Sensor with Langasite, Sensors, 15 (2015) 28531-28542. https://doi.org/10.3390/s151128531

[8] B. V. Lahidjani, H. Badri, A SAW Delay Line Sensor Combined with Micro-hotplate for Bio-chemical Applications, Sens. Transducers.J., 125 (2011) 247–255.

[9] B. François, C. Droit, G. Martin, J-M. Friedt, S. Ballandras,High temperature interrogation unit for wireless SAW-based temperature sensors, Procedia Eng., 25 (2011) 1273–1276. https://doi.org/10.1016/j.proeng.2011.12.314

[10] P. Nicolay, les capteurs à ondes élastiques de surface: applications pour la mesure des basses pressions et des hautes températures, Ph.D. dissertation. Université Henry Poincaré. France, 2007.

[11] G. Bruckner, J. Bardong, Wireless Readout of Multiple SAW Temperature Sensors, Sensors,19 (2019) 3077. https://doi.org/10.3390/s19143077

[12] T. Aubert, Contribution à l'élaboration de capteurs sans-fil opérant à très haute température (500-1000º) à base de dispositifs à ondes élastiques de surface: choix des matériaux constitutifs, Ph.D. dissertation., univ-lorraine. France, 2018.

[13] O. Elmazria, T.Aubert, Wireless SAW sensor for high temperature applications: Material point of view, Int. Soc. Opt. Eng. Proc. SPIE , 8066 (2011). https://doi.org/10.1117/12.889165

[14] M. A. Odintzov, N. I. Sushentzov, L. Kudryavtzev, AlN films for SAW sensors, Sens. Actuator A Phys., 28 (1991) 203–206. https://doi.org/10.1016/0924-4247(91)85008-C

[15] X. Ye, Q. Wang, L. Fang, X. Wang, B. Liang. Comparative Study of SAW Temperature Sensor Based on Different Piezoelectric Materials and Crystal Cuts for Passive Wireless Measurement, SENSORS, 2010 IEEE, Waikoloa, HI, USA, 2010, 585-588. https://doi.org/10.1109/ICSENS.2010.5690462

[16] N. Belkhelfa, R. Serhane, Temporal study of one-port and two-port SAW delay lines for temperature sensing, 2021 Int. Conf. Inf. Syst. Adv. Technol.,Tebessa, Algeria, 2021, 1-5. https://doi.org/10.1109/ICISAT54145.2021.9678459

[17] Z. Zhousheng, R. Guoxing, M. Aiqing, Z. Iu, L. Feng, Design of Passive Wireless resonance type SAW Temperature Sensor, 2014 Int. Conf. Power Syst. Technol., Chengdu, China, 2014, 1451-1456. https://doi.org/10.1109/POWERCON.2014.6993739

[18] Y. Dai , S. Li , Q. Sun , Q. Peng , C. Gui , Y. Zhou , S. Liu. Properties of AlN film grown on Si (111). J. Cryst. Growth., 435 (2016) 76–83. https://doi.org/10.1016/j.jcrysgro.2015.11.016

[19] W. Dong, X. Ji, J. Huang, T. Zhou, T. Li, Y. Fan, K. Xu. Sensitivity enhanced temperature sensor: one-port 2D surface phononic crystal resonator based on AlN/sapphire, Semicond. Sci. Technol., 34 (2019) 055005–055014. https://doi.org/10.1088/1361-6641/ab0a82

[20] Comsol. (2012). MEMS Module User's Guide, Version 4.3a, Part No. CM020801. Available e-mail: HUMANIST@NYVM.ORG Available: https://cdn.comsol.com/doc/4.3/COMSOL_ReleaseNotes.pdf. accessed Jan. 17, 2018

[21] G. Bu, D. Ciplys, M. Shur, L.J. Schowalter, S. Schujman, R. Gaska. On the use of atmospheric plasmas as electromagnetic reflectors, Electron. Lett., 39 (2003) 876–880.

[22] M. B. Schulz, B. J. Matsinger, M. G. Hollan, Temperature Dependence of Surface Acoustic Wave Velocity on α Quartz, J. Appl. Phys., 41 (1970) 2755. https://doi.org/10.1063/1.1659311

[23] J. H. Kuypers, C M. Lin, G. Vigevani, A P. Pisano, Intrinsic Temperature Compensation of Aluminum Nitride Lamb Wave Resonators, 2008 IEEE International Frequency Control Symposium, Honolulu, HI, 2008, 240-249. https://doi.org/10.1109/FREQ.2008.4622998

[24] D.K. Pandey, R.R. Yadav, Temperature dependent ultrasonic properties of aluminum nitride, Appl. Acoust., 70 (2009) 412–415. https://doi.org/10.1016/j.apacoust.2008.05.011

[25] A B. Randles, J M. Tsai, P Kropelnicki, H Cai, Temperature Compensated AlN Based SAW., J. Autom. Control.Eng. 2 (2014) 191- 194. https://doi.org/10.12720/joace.2.2.191-194

[26] N. Belkhelfa, R. Serhane, Silicon SAW parameters extraction and optimization using finite elements analysis, 2019 Int.Conf.Adv. Electr. Eng., Algiers, Algeria, 2019, 1-5. https://doi.org/10.1109/ICAEE47123.2019.9014723